An Analytically Based Pressurised Pipeline Decompression Model

Jiahuan Yi, PhD Student

Haroun Mahgerefteh, Professor of Chemical Engineering

Department of Chemical Engineering, University College London, London, UK WC1E 7JE

This paper describes the fundamental extension of a computationally efficient analytical Vessel Blowdown Model (VBM) for simulating the transient outflow following the accidental failure of high-pressure pipelines transporting condensable gases or fluid mixtures. Based on the modification of the standard vessel discharge equations through incorporating additional mass and energy terms for the inflow, the extended model addresses the fundamental limitations of VBM in handling un-isolated releases and fluid/wall heat exchanges. The new model is successfully tested against the results obtained using an extensively validated but computationally demanding numerical model simulating the failures of a hypothetical pressurised methane pipeline. The validation tests include various puncture diameters, feed flow rates and pipe lengths producing a maximum disagreement of ±7 % between the two models' predictions.

Keywords: process safety, risk assessment, pipeline failure, fluid mechanics, mathematical modelling

1. Introduction

Long pressurised pipelines are extensively employed for transporting large quantities of hydrocarbons. The high pressures involved, combined with the massive flammable inventories, pose significant risks to life and property in the event of pipeline failure (Mahgerefteh *et al.*, 2011). Of the two types of pipeline failures, a through-wall puncture is less catastrophic as compared to a Full Bore Rupture (FBR). However, given that the former is far more frequent (Lydell, 2000), the consequences associated with pipeline puncture failure must be assessed. Central to the above is the accurate prediction of the transient mass discharge rate as this serves as the source term for determining all the conceives associated with pipeline failure, including fires, explosions, environmental pollution and toxic release (Mahgerefteh *et al.*, 2011). Therefore, the development of accurate, robust and efficient mathematical models for predicting the outflow in the event of pipeline puncture failure has been the focus of considerable attention (see for example Chen *et al.*, 1995; Mahgerefteh *et al.*, 1999).

In light of the above, several numerically based pipeline decompression models have been developed. Given that in principle the mathematical problem addressed involves solving the conservation equations of mass, momentum and energy which are a set of coupled, non-linear and high-order partial differential equations usually containing terms that are not analytically solvable, their solutions are sought using numerical techniques (Flatt, 1986). Previous attempts include a Finite Difference Method (FDM) (Bendiksen *et al.*, 1991; Chen, 1993), a Finite Element Method (FEM) (Bisgaard *et al.*, 1987; Lang, 1991) and the Method of Characteristic (MOC) (Chen *et al.*, 1992; Olorunmaiye and Imide, 1993; Mahgerefteh *et al.*, 1999). Given that these methods invariably involve the numerical discretisation of the pipeline into a number of small elements, they all share the fundamental drawback of long computational runtimes (Mahgerefteh *et al.*, 2011). For a typical 100 km, 800 mm i.d. natural gas pipeline experiencing a 20 mm puncture, for example, the CPU time for simulating its complete decompression typically range from days to weeks depending on the computer processing speed employed.

To address the above problem, a number of authors have proposed simplistic pipeline decompression models. Some important attempts include a unified outflow model (Norris and Puls, 1993; Norris, 1994), a quasi-steady state model (Webber *et al.*, 1999) and a Vessel Blowdown Model (VBM) (Mahgerefteh *et al.*, 2011). These models were developed mainly based on steady state flow assumption for which analytical solutions can be obtained, largely addressing the issue of long computational runtimes associated with numerically based techniques (e.g. FEM, FDM and MOC) used for simulating pipeline puncture failure. However, the range of applicability of the unified outflow model remains unclear and the quasi-steady state model is limited to simulating pure components.

VBM is the most recent attempt to address these limitations. In this model, the transient outflow from a punctured pipeline is approximated as that emanating from a vessel. The model adopts the classic vessel discharge equations (Coulson *et al.*, 1999) to simulate the flow dynamics. This essentially defines the decompression from a pipe as a solely time-dependent process requiring no numerical discretisation of the pipe length for seeking solutions to the flow equations. Given this, the CPU times are drastically reduced to a negligible level. For example, the simulation of the complete depressurisation of a 5 km length, 300 mm i.d. pipeline containing equi-molar methane and pentane following a 120 mm puncture takes ca. 1 s on a 2.66 GHz, 3.0 GB RAM computer (Mahgerefteh *et al.*, 2011).

VBM is verified against an extensively validated numerical model (Mahgerefteh *et al.*, 1999) and displays little loss of accuracy in simulating punctures smaller than 40 % of pipe internal diameter. However, despite its success, VBM cannot handle the highly plausible pipeline failure scenario involving un-isolated release where pumping of the pressurised inventory continues despite puncture. In addition, given its isothermal bulk flow assumption, fluid/wall heat exchanges are ignored, limiting its applicability.

This paper describes the development and testing of a new efficient analytically based pipeline puncture model addressing the above limitations of VBM. The model approximates the transient outflow from an un-isolated pipeline as the blowdown from a vessel with inflow. The fluid flow equations are modified from the standard vessel discharge equations (Coulson *et al.*, 1999) by incorporating additional mass and energy terms accounting for the effect of inflow. The fluid/wall friction effect is accounted for by a correlation used for calculating the pressure drop for isothermal steady state flow (Mahgerefteh *et al.*, 1999). This, along with the assumption that the flow inside the pipe remains quasi-steady state during decompression, is employed to evaluate the flow conditions upstream the puncture which in turn serve as the boundary conditions for modelling

the transient mass discharge rate following pipeline failure. The model is tested against an extensively validated but computationally demanding numerically based pipeline decompression model (Mahgerefteh *et al.*, 1999) based on the failure of a hypothetical un-isolated pipeline containing pure methane initially at 21 bar and 300 K. The simulation runs are based on a midway puncture covering a wide range of pipeline failure scenarios varying inflow rate (1 to 7.5 kg/s), pipe length (100 to 5000 m) and puncture to pipe internal diameter ratio (0.2 to 0.8). Following its testing, the CPU times of the new model for simulating the above failure scenarios are compared against those obtained using the numerically based model.

2. Theory

2.1 The numerically based model

The analytically based pipeline decompression model described in the following sections 2.2 to 2.4 is tested against a numerically based model, the full details of which are given elsewhere (Mahgerefteh *et al.*, 1999). Hence, only a brief account is given below.

In establishing the fluid dynamics, the model adopts 1-D flow and Homogeneous Equilibrium Mixture (HEM) assumptions. The resulting flow conservation equations of mass, momentum and energy are given by:

$$\frac{\partial \rho}{\partial t} + \frac{\partial \rho u}{\partial x} = 0 \tag{1}$$

$$\frac{\partial \rho u}{\partial t} + \frac{\partial (\rho u^2 + P)}{\partial x} = \beta - \rho g \sin\theta \tag{2}$$

$$\frac{\partial \rho E}{\partial t} + \frac{\partial (\rho u E + P u)}{\partial x} = \beta u - \rho u g \sin\theta + Q_h \tag{3}$$

where, ρ, u, P and E are the density, velocity, pressure and energy, respectively. β, g, θ and Q_h respectively denote the fluid/wall friction, gravitational acceleration, angle of the pipe relative to the horizontal and heat transferred across the pipe wall to the fluid.

The numerical solution of the set of the above quasi-linear hyperbolic equations (1) to (3) is performed using MOC (Hoffman and Zucrow, 1976) involving the numerical discretisation of the pipeline into a sufficiently large number of space and time elements. This method intrinsically handles the choked flow at the pipe ruptured end via the Mach line characteristics. Therefore, it is considered more accurate than other numerical schemes (e.g. FEM, FDM) in dealing with fast transient flows which are often encountered during pipeline decompression (Mahgerefteh *et al.*, 1999). The fluid phase equilibrium data are computed using the widely applied Peng-Robinson Equation of State (PR EoS) (Peng and Robinson, 1976). The heat transfer and friction effects are determined by well-established flow- and phase-dependent correlations for hydrocarbon mixtures, resulting in a better prediction of the fluid temperature especially in the latter stages of depressurisation where fluid/wall heat transfer effects become important. The use of interpolation grid (Mahgerefteh *et al.*, 2007), serving as a look-up table for computing fluid thermodynamic properties, significantly reduces the number of flash calculation involved and hence the computational runtimes. Following the development of this model, carrying out simulations involving pipeline decompression accurately became possible on personal computers for the first time. However, despite this, its computational workload can drastically increase for simulating long pipelines. This makes the use of this model unfavourable when design and safety assessment of long pipelines are concerned.

The above numerical model has been extensively validated against a broad range of field data (see for example Chen, 1993; Richardson, S.M. and Saville, 1996). Full details of its validation can be found elsewhere (see for example Mahgerefteh *et al.*, 1999). For brevity only a brief account is given here. Figure 1 shows the comparison between the simulated and measured data for pressure-time profile at both the pipe open and intact ends during the Isle of Grain P40 (FBR) decompression test. As may be observed, the simulated pressure profiles in general present close agreement to the measured data at both open and intact ends of the test pipe throughout decompression. The initial sudden pressure drop as a result of the instantaneous phase-transition from liquid to two-phase mixture is accurately predicted. The above is followed by a much lower rate of decompression where the maximum discrepancy between the simulated and measured pressure data is ca. 0.4 bar.

Figures 2 (a) and (b) respectively present the simulated and measured pressure variations as a function of time during decompression for the Isle of Grain P45 (75 mm puncture) and P47 (50 mm puncture) tests. Again relatively good agreement between experimental and simulated data is evident.

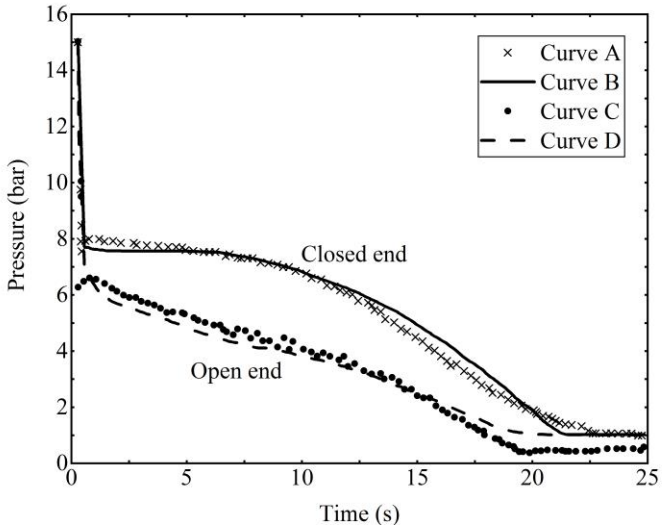

Figure 1. Pressure-time profiles at closed and open ends for the Isle of Grain P40 FBR test. Curve A: Field data (closed end); Curve B: Simulated data (closed end); Curve C: Field data (open end); Curve D: Simulated data (open end).

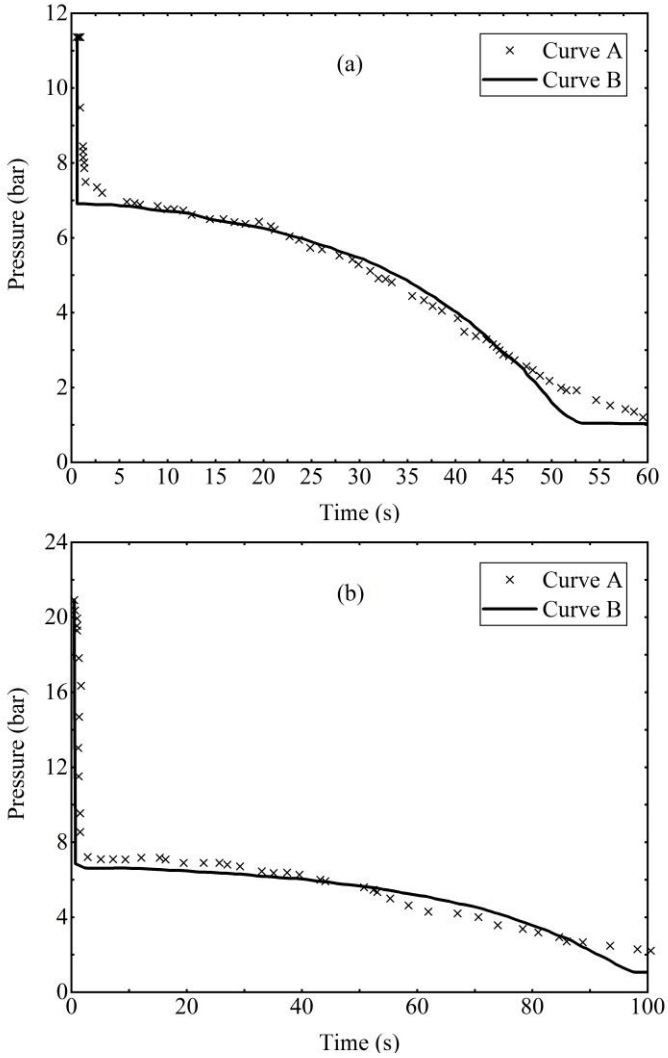

Figure 2. Pressure-time profiles for the Isle of Grain P45 (a) and P47 (b) puncture test. Curve A: Field data; Curve B: Simulated data.

2.2 Discharge model

A schematic representation of the outflow from a horizontal pressurised pipeline is given in figure 3, indicating the pertinent fluid properties used in the mathematical development of the new analytically based pipeline decompression model.

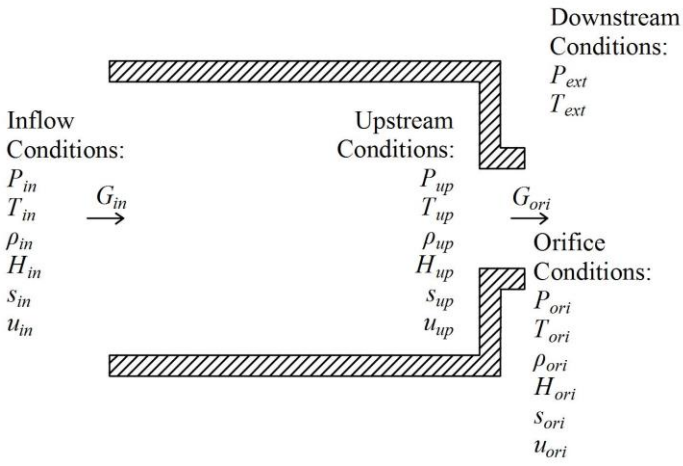

Figure 3. Schematic representation of the outflow from a horizontal pressurised pipeline indicating the pertinent fluid properties required for the mathematical development of the new analytically based pipeline decompression model.

In order to avoid numerical discretisation in solving the flow equations to maintain a high level of computational efficiency, the standard analytically based vessel discharge equations adapted for HEM assumption (Martynov *et al.*, 2014) incorporating additional mass and energy terms for inflow are employed to describe the outflow from a horizontal pressurised pipeline following its failure. The resulting conservation equations of mass and energy written in integral form are given by:

$$\frac{dM}{dt} = G_{in} - G_{ori} \tag{4}$$

$$\frac{dME}{dt} = G_{in}H_{in} - G_{ori}H_{ori} + Q_h \tag{5}$$

where, M, E, G_{in} and G_{ori} are the mass of the fluid in the pipe, specific total energy of the fluid in the pipe, the mass flow rate at the inlet and the mass flow rate at the orifice, respectively. H_{in} and H_{ori}, on the other hand, are the specific total enthalpy of the flow at the inlet and at the orifice, respectively.

The fluid/wall heat exchange term, Q_h is defined as:

$$Q_h = \frac{4}{D}U_h(T_{ext} - T_f) \tag{6}$$

where, D, U_h, T_{ext} and T_f are the pipe internal diameter, overall heat transfer coefficient, ambient temperature and fluid temperature, respectively.

2.3 Physical properties

The fluid thermodynamic properties and phase equilibrium data are calculated using the PR EoS (Peng and Robinson, 1976) as it is considered particularly applicable to high-pressure, multi-component hydrocarbons (Mahgerefteh *et al.*, 2011). The number of fluid phases presented in the flow during pipeline decompression is determined by the stability test based on the Gibbs tangent plane criterion (Michelsen, 1982). The fluid properties of a two-phase mixture are handled based on the HEM assumption; that is, the pressure, temperature and velocity are identical across phases and the pseudo properties including the heat capacity, specific volume, energy and entropy of two-phase mixtures are calculated based on mass-averaged pure liquid and pure gas properties obtained from PR EoS, given by:

$$\phi_m = \phi_g\chi + \phi_l(1 - \chi) \tag{7}$$

where, ϕ_m, ϕ_g and ϕ_l are the mass-specific properties of a two-phase mixture and its constituent saturated vapour and liquid phases, respectively. χ is the fluid quality.

The local speed of sound, c and φ for single-phase fluids is determined analytically (Groves *et al.*, 1978; Picard and Bishnoi, 1988), given by:

$$c^2 = \frac{\gamma}{k\rho} \tag{8}$$

$$\varphi = \frac{\rho\xi T c^2}{C_p} \tag{9}$$

where, γ, ρ, T and C_p are the ratio of specific heats, fluid density, fluid temperature and isobaric specific heat capacity, respectively. k and ξ are the isothermal and isobaric coefficients of volumetric expansion, respectively.

For two-phase mixtures, defining γ and C_p becomes complicated (Mahgerefteh *et al.*, 1999) and the speed of sound, c and φ are evaluated numerically, given by:

$$c^2 = \frac{\Delta P}{\rho(T,P)_s - \rho(T^*, P-\Delta P)_s} \tag{10}$$

$$\varphi = \rho^2 \left(\frac{\Delta T}{\Delta \rho}\right)_s \tag{11}$$

where, the subscript, s denotes the isentropic condition.

Equation (12) is solved for T^* iteratively using Newton-Raphson method with the following objective function, ω:

$$\omega^{(n)} = s(T,P)_s - s(T^{*(n)}, P-\Delta P)_s \tag{12}$$

where, the superscript, n denotes the iteration level.

2.3 Initial conditions

Due to fluid/wall friction, the presence of inflow leads to pressure drop inside the pipe resulting in the variation of fluid properties along the pipe (Menon, 2005). In the present study, the flow in the pipe is taken to be isothermal steady state prior to pipeline failure. The corresponding pressure drop between two given locations along the pipe, denoted by 1 and 2 respectively, is given by (Mahgerefteh *et al.*, 1999):

$$P_2 = P_1 + \frac{\beta_1}{\left[1 - \frac{u^2}{zRT}\right]_1}(x_2 - x_1) \tag{13}$$

where, z and R are the compressibility factor and gas constant, respectively.

The friction force term, β is defined as:

$$\beta = -2\frac{f}{D}\rho u|u| \tag{14}$$

where, f denotes the Fanning friction factor, which is determined as follows.

For transition and turbulent flows ($Re > 2000$), it is calculated using Chen's correlation (Chen, 1979) given its simple analytical form and high accuracy when compared to Colebrook correlation (Colebrook, 1939) which is accepted as the benchmark in Fanning friction factor predictions (Ouyang and Aziz, 1996), given by:

$$\frac{1}{\sqrt{f}} = 3.48 - 1.7372\ln\left(\frac{\varepsilon}{Ra} - \frac{16.2446}{Re}\ln\left(\frac{\left(\frac{\varepsilon}{Ra}\right)^{1.0198}}{6.0983} + \left(\frac{7.149}{Re}\right)^{0.8981}\right)\right) \tag{15}$$

For laminar flows ($Re < 2000$), the Fanning friction factor is calculated using the following well-established correlation:

$$f = \frac{16}{Re} \tag{16}$$

where, ε and Ra are the pipe wall roughness and pipe internal radius, respectively. The Reynold's number, Re is defined as:

$$Re = \frac{\rho u D}{\mu} \tag{17}$$

where, μ is the fluid viscosity, which is determined as follows.

For single-phase fluids, the viscosity is calculated using the Ely and Hanley scheme for gas and the Dymond and Assael scheme for liquid (Massey, 1983). For two-phase mixtures, the viscosity is determined based on mass-averaged pure liquid and pure gas properties (Mahgerefteh *et al.*, 1999), given by:

$$\frac{1}{\mu_m} = \frac{\chi}{\mu_g} + \frac{(1-\chi)}{\mu_l} \tag{18}$$

2.4 Boundary conditions

The present study assumes that the flow inside the pipe remains quasi-steady state following pipeline failure. By making this assumption, equation (13) (described in section 2.3) used for calculating the pressure drop for steady state flow can then be applied to calculate the instant fluid conditions upstream the orifice during decompression. This assumption was previously adopted by Webber *et al.* (1999) in the development of a two-phase discharge model for pipeline FBR and was found to have good validity following the model's validation against the Isle of Grain P40 test (Richardson, S.M. and Saville, 1996).

The orifice flow conditions are determined using the steady state 'straw method' (Morin *et al.*, 2012). The feed flow rate is assumed to be constant during depressurisation.

3. Results and Discussion

3.1 Case study

The efficacy of this new analytically based pipeline decompression model described in sections 2.2 to 2.4 is tested against the rigorously validated numerically based model (Mahgerefteh *et al.*, 1999) described in section 2.1 using a hypothetical 300 mm i.d. thermally insulated pipeline containing pure methane. The relevant pipeline characteristics and prevailing conditions are summarised in table 1. The failure location is assumed to be the midway along the pipeline. The tests involve simulating un-isolated release covering several realistic failure scenarios. For the simulations using the numerically based model, an automatic nested grid system (Mahgerefteh *et al.*, 1999) applying finer numerical discretisation near the puncture is used. For simplicity, a discharge coefficient of unity is assumed.

Table 1. Pipeline characteristics and prevailing conditions.

Parameter		**Value**
Pipe characteristics	Pipe internal diameter (mm)	300
	Pipe wall thickness (mm)	10
	Pipe roughness (mm)	0.05
	Heat transfer coefficient (W/m^{2}K)	5
Inlet conditions	Feed composition (mol %)	Methane 100 %
	Feed pressure (bar)	21
	Feed temperature (K)	300
Failure parameters	Puncture location	Mid-length
	Discharge coefficient	1
Ambient conditions	Ambient pressure (bar)	1.01
	Ambient temperature (K)	290

3.2 Different feed flow rates

Figure 4 shows the simulated mass discharge rate variations with time following a 60 mm puncture predicted by both models. The data points and solid lines are respectively the predictions of the numerical and analytical models. The simulated results are produced for pipeline feed flow rates ranging from 1 to 7.5 kg/s.

As can be observed, the analytical model produces generally good agreement with the numerical model predictions indicating minor discrepancies throughout. As the decompression continues, the mass discharge rate decreases more slowly with time in the case of a higher inflow rate. A reason for this is that a higher inflow rate which provides more compensation for the inventory would essentially maintain the pressure inside the pipe at a higher level, therefore leading to a slower rate of decompression. It should be noted that the mass discharge rate will eventually reach the initial feed flow rate.

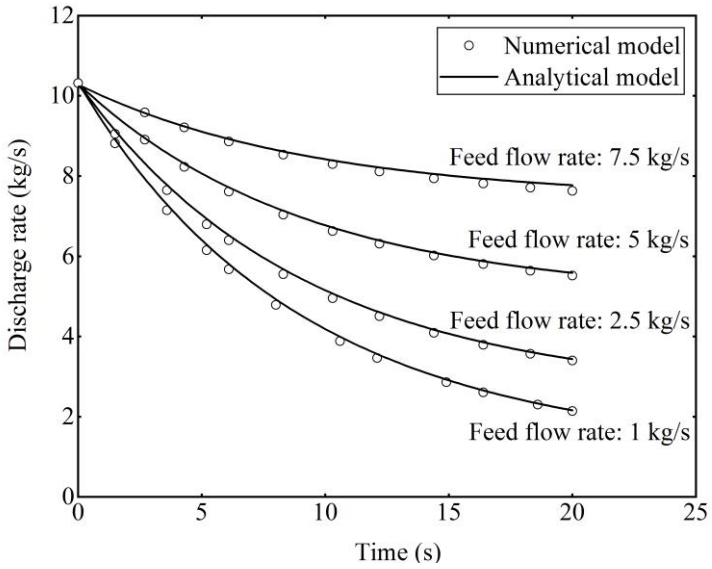

Figure 4. Comparison of the mass discharge rate variation with time at the orifice based on the predictions of the numerical (data points) and analytical (solid lines) models for different feed flow rates (Puncture/pipe internal diameter ratio: 0.2; Pipe length: 100 m).

3.3 Different pipe lengths

The following examines the efficacy of this new model in handling pipelines of various lengths. Figure 5 shows the mass discharge rate variations with time following a 60 mm puncture predicted by both models. The data points and solid lines are respectively the predictions of the numerical and analytical models. The results are determined for different pipe lengths; 500, 1000, 2500 and 5000 m. A feed flow rate of 2.5 kg/s is assumed in all cases. Other pipeline characteristics and prevailing conditions used for the simulations are summarised in table 1.

Once again, relatively good agreement between the predictions of the numerical and analytical models is obtained for all lengths tested. The profiles display similar trends as those in figure 4. As the pipe length increases, the mass discharge rate decrease more slowly with time. Given that a longer pipeline contains a larger amount of inventory, it is therefore capable of maintaining the pressure inside the pipe for a longer duration following pipeline failure. This in turn would lead to a slower decompression rate as compared to a shorter pipeline.

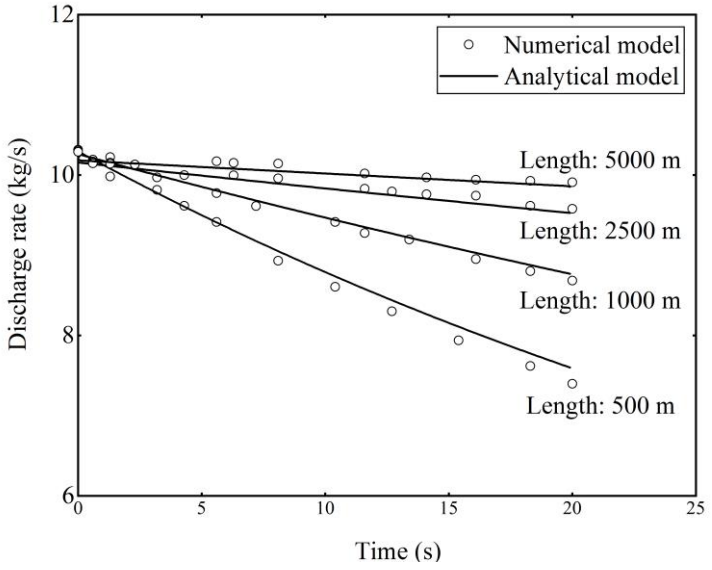

Figure 5. Comparison of the mass discharge rate variation with time at the orifice based on the predictions of the numerical (data points) and analytical (solid lines) models for different pipe lengths (Puncture/pipe internal diameter ratio: 0.2; Feed flow rate: 2.5 kg/s).

3.4 Different puncture diameters

This section primarily investigates the capability of the present model in handling relatively large punctures. The failure scenarios investigated include 180 and 240 mm punctures, respectively corresponding to 60 and 80 % of the pipe internal diameter. Figures 6 (a) and (b) respectively present the simulated mass discharge rate-time profiles from both models for the 180 and 240 mm puncture scenarios. The results are determined for a 100 m length pipe with 2.5 kg/s feed flow rate. Other pipeline characteristics and prevailing conditions used for the simulations are presented in table 1.

For both puncture size scenarios investigated, generally good agreement is obtained between the two predictions with the new analytical model underestimating the mass discharge rate by ca. 2.6 and 6.9 % for the 180 and 240 mm punctures respectively as compared to the numerical model. This is considered a substantial improvement to VBM where punctures larger than 40 % of the pipe internal diameter cannot be handled (Mahgerefteh *et al.*, 2011). Such a limitation of VBM could be due its isothermal bulk flow assumption which ignores the fluid/wall heat exchanges during pipeline decompression. When the puncture size increases, such an assumption becomes increasingly inapplicable given the much quicker decompression involved which leads to rapid cooling inside the pipe.

However, the discrepancy between the predictions of both models increases with increasing puncture size (ca. 2.6 and 6.9 % for 180 and 240 mm puncture scenarios respectively). This is probably due to the different magnitudes of fluid/wall friction involved. A larger puncture leads to a higher acceleration of the fluid upstream the orifice thus resulting in increase in the frictional losses. However, given that the present model assumes quasi-steady flow, such frictional losses and hence the corresponding energy losses are not taken into consideration. Consequently, the above assumption becomes increasingly inapplicable with increase in puncture diameter thus leading to increased simulation errors.

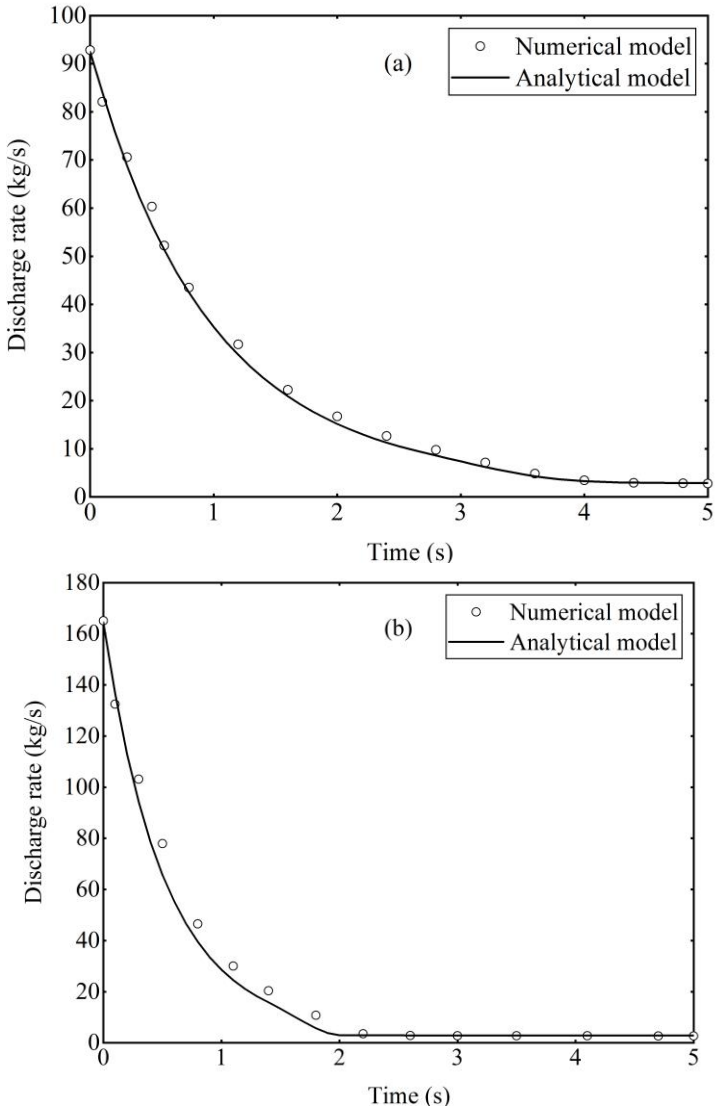

Figure 6. Comparison of the mass discharge rate variation with time at the orifice based on the predictions of the numerical (data points) and analytical (solid lines) models for 180 (a) and 240 (b) mm punctures (Pipe length: 100 m; Feed flow rate: 2.5 kg/s).

3.5 Analysis of computational runtimes

Table 2 presents the comparison of the computational runtimes between the numerical and analytical models for simulating pipeline failures. The simulations involve the complete decompression of several isolated pipelines with different lengths, including 100, 1000 and 5000 m. The selected puncture diameter for these simulations is 60 mm. All other input conditions used are summarised in table 1. These simulations are performed using a 3.80 GHz, 16.0 GB RAM computer.

Table 2. Comparison of the computational runtimes between the numerical and analytical models.

Pipe length (m)	**Computational runtimes**		
	Numerical model	*Analytical model*	*% of reduction*
100	1 min 41 s	6.63 s	93.44 %
1000	16 min 37 s	55.89 s	94.39 %
5000	2 hr 34 min 59 s	4 min 6 s	97.35 %

As can be observed from table 2, the computational runtimes using the new analytical model are significantly lower than those based on the numerical model for all pipe lengths simulated. Such reductions are even more notable in the case of longer pipelines. This makes the application of this new model to simulating long pipelines particularly attractive.

4. Conclusions

The development and testing of an efficient analytically based pipeline decompression model was described. The model addresses the limitations of a previously developed analytically based VBM in handling un-isolated releases and fluid/wall heat exchanges. The model is developed based on incorporating additional mass and energy terms accounting for the inflow into the standard vessel discharge equations. Given that the resulting equations may be solved analytically, the fundamental drawback of long computational runtimes associated with numerically based pipeline decompression models has been addressed.

The model developed is tested against the predictions using an extensively validated numerically based pipeline decompression model by using a hypothetical un-isolated methane pipeline covering a wide range of failure scenarios as a case study. These include different pipe feed flow rates, pipe lengths and puncture diameters. The results show that the new analytical model generally produces good agreement with the numerical model predictions in simulating un-isolated releases at a fraction of the computation runtime.

A particularly important finding based on the above tests is that the new analytical model handles relatively larger punctures (up to 80 % of the pipe internal diameter) quite well. This is a substantial improvement to VBM where only punctures smaller than 40 % of the pipe internal diameter can be handled. This improvement is a consequence of the fact that the new model accounts for fluid/wall heat exchanges which become significant for large diameter punctures. However, the accuracy of the new model decreases with the increase of the puncture size. This could be due to the increasing incapability of the quasi-steady state assumption, which ignores the growing influence of fluid/wall frictional effects in the vicinity of the puncture as its diameter increases.

Future study will focus on extending the model to simulate realistic scenarios such as time varying feed flow rates and different upstream conditions such as infinite reservoirs.

Nomenclature

A – area, m^2;

c – local speed of sound, m/s;

C_D – discharge coefficient;

C_p – isobaric specific heat capacity, J/(kg·K);

D – pipe internal diameter, m;

E – specific total energy, J/kg;

f – Fanning friction factor;

G – mass flow rate, kg/s;

g – gravitational acceleration, m/s^2;

H – specific total enthalpy, J/kg;

h – specific enthalpy, J/kg;

k – isothermal coefficient of volumetric expansion, K^{-1};

M – mass of the fluid in the pipe, kg;

P – pressure, Pa;

Q_h – heat transferred across the pipe wall to the fluid, J/kg;

R – gas constant, J/(mol·K);

Ra – pipe internal radius, m;

s – specific entropy, J/(kg·K);

t – time, s;

T – temperature, K;

u – velocity, m/s;

U_h – overall heat transfer coefficient, W/(m^2·K);

x – distance, m;

z – compressibility factor

Greek letters:

γ – ratio of specific heats;

θ – angle of the pipe relative to the horizontal, rad;

μ – viscosity, kg/(m·s);

ξ - isobaric coefficient of volumetric expansion, K^{-1};

ρ – density, kg/m^3;

χ – fluid quality

Subscripts:

ext – ambient;

g – vapour phase;

in – inlet;

l – liquid phase;

m – two-phase mixture;

ori – orifice

References

Bendiksen, K. H. *et al.* (1991) 'The Dynamic Two-Fluid Model OLGA: Theory and Application', *SPE Production Engineering*. Edinburgh: Institution of Chemical Engineers (IChemE), 6(2), pp. 171–180. doi: 10.2118/19451-PA.

Bisgaard, C., Sørensen, H. H. and Spangenberg, S. (1987) 'A finite element method for transient compressible flow in pipelines', *International Journal for Numerical Methods in Fluids*, 7(3), pp. 291–303. doi: 10.1002/fld.1650070308.

Chen, J. R. (1993) *Modelling of transient flow in pipeline blowdown problems*. Imperical College London.

Chen, J. R., Richardson, S. M. and Saville, G. (1992) 'Numerical simulation of full-bore ruptures of pipelines containing perfect gases', *Transactions of the Institution of Chemical Engineers. Part B*, 70, p. 59.

Chen, J. R., Richardson, S. M. and Saville, G. (1995) 'Modelling of two-phase blowdown from pipelines-I. A hyperbolic model based on variational principles', *Chemical Engineering Science*, 50(4), pp. 695–713. doi: 10.1016/0009-2509(94)00246-N.

Chen, N. H. (1979) 'An Explicit Equation for Friction Factor in Pipe', *Industrial and Engineering Chemistry Fundamentals*, 18(3), pp. 296–297. doi: 10.1021/i160071a019.

Colebrook, C. F. (1939) 'Turbulent flow in pipes with particular reference to transition region between the smooth and rough pipe laws', *Journal of the Institution of Civil engineers*, 12(8), pp. 393–422.

Coulson, J. M. *et al.* (1999) *Chemical Engineering Volume 1: Fluid Flow , Heat Transfer And Mass Transfer*. Butterworth-Heinemann.

Flatt, R. (1986) 'Unsteady compressible flow in long pipelines following a rupture', *International Journal for Numerical Methods in Fluids*, 6(2), pp. 83–100. doi: 10.1002/fld.1650060204.

Groves, T. K., Bishnoi, P. R. and Wallbridge, J. M. E. (1978) 'Decompression wave velocities in natural gases in pipe lines', *The Canadian Journal of Chemical Engineering*, 56(6), pp. 664–668. doi: 10.1002/cjce.5450560602.

Hoffman, J. D. and Zucrow, M. J. (1976) *Gas dynamics*. Wiley.

Lang, E. (1991) 'Gas flow in pipelines following a rupture computed by a spectral method', *ZAMP Zeitschrift f*[illegible]*r angewandte Mathematik und Physik*, 42(2), pp. 183–197. doi: 10.1007/BF00945792.

Lydell, B. O. Y. (2000) 'Pipe failure probability—the Thomas paper revisited', *Reliability Engineering & System Safety*, 68(3), pp. 207–217. doi: 10.1016/S0951-8320(00)00016-8.

Mahgerefteh, H., Atti, O. and Denton, G. (2007) 'An Interpolation Technique for Rapid CFD Simulation of Turbulent Two-Phase Flows', *Process Safety and Environmental Protection*, 85(1), pp. 45–50. doi: 10.1205/psep.05118.

Mahgerefteh, H., Jalali, N. and Fernandez, M. I. (2011) 'When does a vessel become a pipe?', *AIChE Journal*, 57(12), pp. 3305–3314. doi: 10.1002/aic.12541.

Mahgerefteh, H., Saha, P. and Economou, I. G. (1999) 'Fast numerical simulation for full bore rupture of pressurized pipelines', *AIChE Journal*, 45(6), pp. 1191–1201. doi: 10.1002/aic.690450605.

Martynov, S. *et al.* (2014) 'Modelling three-phase releases of carbon dioxide from high-pressure pipelines', *Process Safety and Environmental Protection*. Institution of Chemical Engineers, 92(1), pp. 36–46. doi: 10.1016/j.psep.2013.10.004.

Massey, B. S. (1983) *Mechanics of Fluids*. Wokingham: Van Nostrand Reinhold.

Menon, E. S. (2005) *Gas pipeline hydraulics*. Crc Press.

Michelsen, M. L. (1982) 'The isothermal flash problem. Part I. Stability', *Fluid Phase Equilibria*, 9(1), pp. 1–19. doi: 10.1016/0378-3812(82)85001-2.

Morin, A., Kragset, S. and Munkejord, S. T. (2012) 'Pipeline flow modelling with source terms due to leakage: The straw method', *Energy Procedia*, 23(1876), pp. 226–235. doi: 10.1016/j.egypro.2012.06.023.

Norris, H. L. (1994) 'Hydrocarbon Blowdown From Vessels and Pipelines', in *SPE Annual Technical Conference and Exhibition*. Society of Petroleum Engineers. doi: 10.2118/28519-MS.

Norris, H. L. and Puls, R. C. (1993) 'Single-Phase or Multiphase Blowdown of Vessels or Pipelines', in *SPE Annual Technical Conference and Exhibition*. Society of Petroleum Engineers. doi: 10.2118/26565-MS.

Olorunmaiye, J. A. and Imide, N. E. (1993) 'Computation of natural gas pipeline rupture problems using the method of characteristics', *Journal of Hazardous Materials*, 34(1), pp. 81–98. doi: 10.1016/0304-3894(93)87005-E.

Ouyang, L. B. and Aziz, K. (1996) 'Steady-state gas flow in pipes', *Journal of Petroleum Science and Engineering*, 14(3–4), pp. 137–158. doi: 10.1016/0920-4105(95)00042-9.

Peng, D. Y. and Robinson, D. B. (1976) 'A New Two-Constant Equation of State', *Industrial and Engineering Chemistry Fundamentals*, 15(1), pp. 59–64. doi: 10.1021/i160057a011.

Picard, D. J. and Bishnoi, P. R. (1988) 'The importance of real-fluid behavior and nonisentropic effects in modeling

decompression characteristics of pipeline fluids for application in ductile fracture propagation analysis', *The Canadian Journal of Chemical Engineering*, 66(1), pp. 3–12. doi: 10.1002/cjce.5450660101.

Press, W. H. (1992) *Numerical recipes in Fortran 77: the art of scientific computing*. Cambridge university press.

Richardson, S.M. and Saville, G. (1996) *Isle of Grain pipeline depressurisation tests*. HSE Books.

Webber, D. M., Fannelop, T. K. and Witlox, H. W. M. (1999) 'Source terms from two-phase flow in long pipelines following an accidental breach', in *International Conference and Workshop on Modelling the Consequences of Accidental Releases of Hazardous Materials, CCPS*. San Francisco: AIChE, pp. 145–168.